

# Density Functional Theory Study on the Ultrathin InAs/GaAs Core/Shell Nanowires for Solar Cell Applications

Q G Jiang<sup>1, a</sup> and Z M Ao<sup>2, b</sup>

<sup>1</sup> College of Mechanics and Materials, Hohai University, Nanjing 210098, China

<sup>2</sup> Institute of Environmental Health and Pollution Control, School of Environmental Science and Engineering, Guangdong University of Technology, Guangzhou, 510006, China

<sup>a</sup>[jiangqg@hhu.edu.cn](mailto:jiangqg@hhu.edu.cn),

<sup>b</sup>[zhimin.ao@gdut.edu.cn](mailto:zhimin.ao@gdut.edu.cn)

**Abstract.** We have investigated the band structure and charge distributions of very tiny InAs/GaAs core/shell nanowires in wurtzite structure by using first principles calculations, which indicates that the electrons and holes are spatially localized at the GaAs-shell and InAs-core regions, respectively. In addition, the band gaps of the studied core/shell nanowire are close to the optimum band gap for a single-junction solar cell of about 1.5 eV. Furthermore, the band structure of the C<sub>2</sub>S<sub>2</sub> nanowire (with two InAs layers and two GaAs layers) varies significantly with applied axial strain and the charge carriers keep separated when the applied strain is in the range of -2.6% to 3.9%, which is important for the application of solar cells. Our results indicate that InAs/GaAs core/shell nanowires should be a suitable candidate for solar cells.

## 1. Introduction

Recently, solar cells based on GaAs nanowires (NWs) have attracted great interests [1-3]. However, the increased recombination of photogenerated charge carriers and the larger band gap of NWs due to the quantum confinement limit the energy conversion efficiency [4]. The core/shell nanowires (CSNWs) provide a route for charge spatial confinement and band gap engineering. Generally, epitaxial layers with larger band gap act as a barrier to prevent carriers from recombining at the surface. The band gap of bulk GaAs is 1.42 eV [5], while bulk InAs has a much smaller band gap of 0.54 eV [5]. Therefore, InAs is considered to decorate into GaAs nanowire as a core material to form InAs/GaAs CSNWs to realize charge spatial confinement and band gap engineering. InAs/GaAs CSNWs in wurtzite structure were synthesized experimentally [6-8]. However, previous studies mostly focused on the electronic properties of pure InAs and pure GaAs NWs [9,10], while density functional theory (DFT) studies on the electronic structure of InAs/GaAs CSNWs are lack. It is known that the electronic structure of NWs is sensitive to the strain conditions, making strain a useful and economic method to modulate the band structure [11-13]. The band offset of CSNWs has been reported to change significantly under axial strain [14,15]. It is thus essential to gain a basic physical understanding of the effects of the strain field on the band offset of the InAs/GaAs CSNWs to design and optimize the corresponding electronic nanodevices.



In this paper, the atomic structure and electronic properties of InAs/GaAs CSNWs will be studied by using first principles calculations. The effect of axial strain will be also investigated to provide fundamental information for the band structure engineering of InAs/GaAs CSNWs.

## 2. Computational Methods

The simulation is carried out by using DFT [16,17] in this work, which is run in DMol<sup>3</sup> code [18,19]. The generalized gradient approximation (GGA) functional with the PW91 method [20] is used as the exchange-correlation functional. DFT Semi-core Pseudopotentials (DSPP) [16], which replaces core electrons by a single effective potential and introduces some relativistic effects into the core [21], is used for core treatment. In addition, Double Numerical plus Polarization (DNP) [22,23] is chosen as the basis set with orbital cutoff of 4.6 Å. A smearing value of 0.005 Ha (1 Ha = 27.2114 eV) is used. The convergence tolerance of energy is  $1.0 \times 10^{-5}$  Ha, maximum force is 0.002 Ha/Å, and maximum displacement is 0.005 Å in the geometry optimization.

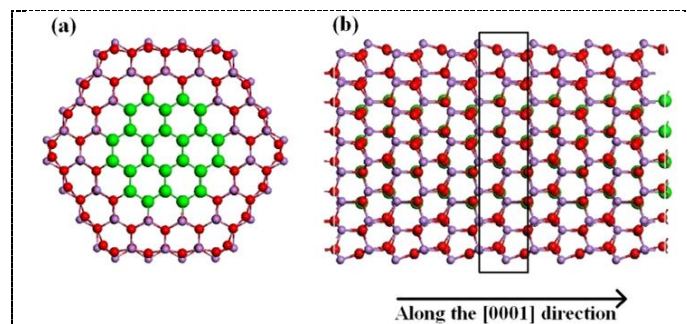


Figure 1. (a)Top and (b) side views of atomic structure of C<sub>2</sub>S<sub>2</sub> CSNW along the [0001] direction, where the small (pink), middle (red) and large (green) spheres represent As, Ga and In atoms, respectively.

The calculated parameters for the bulk InAs and GaAs in wurtzite structures are  $a = 4.361$  (4.041) Å and  $c = 7.195$  (6.679) Å, being consistent with previous DFT calculations [24]. InAs and GaAs usually exhibit the wurtzite structure when their diameters ( $D$ ) are in nanosizes [25,26]. The CSNW is taken along the [0001] axial direction with a hexagonal cross section, as shown in Figure 1a. Because the surface of NWs prepared using molecular beam epitaxy method are not passivated [27], the CSNWs adopt unpassivated but fully reconstructed surface facets. The InAs/GaAs CSNWs are labelled with C<sub>*m*</sub>S<sub>*n*</sub>, where  $m$  and  $n$  denote the number of InAs and GaAs layers, respectively. The axial lattice constants of the relaxed CSNWs are listed in Table 1, which are both smaller than that of bulk InAs and larger than that of bulk GaAs due to the lattice mismatch between InAs and GaAs, *i.e.*, a compression for the InAs-core while a tension for the GaAs-shell.

## 3. Results and Discussions

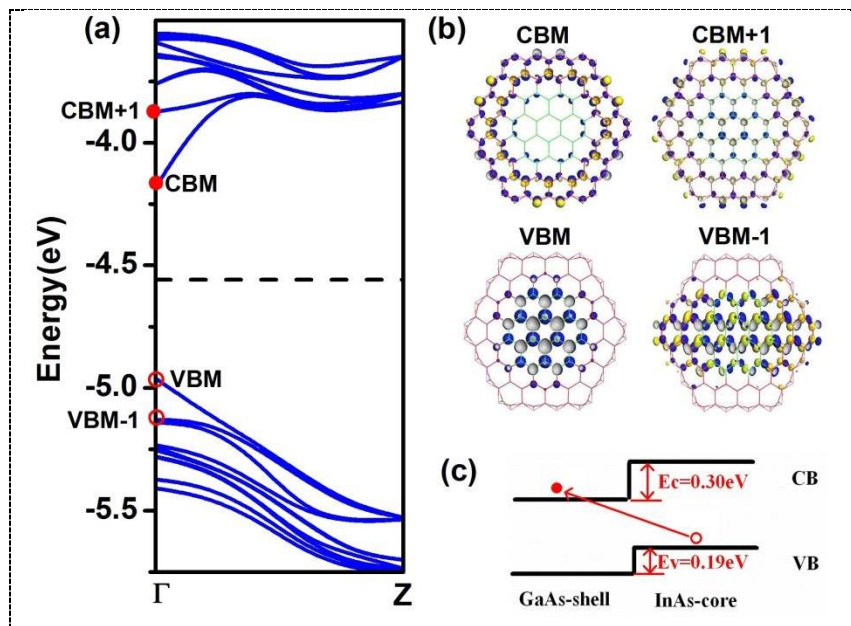


Figure 2. (a) Band structure of  $C_2S_2$  CSNW, where the energy levels of CBM+1, CBM, VBM and VBM-1 states are labelled with red circles. The dash line represents the Fermi level. (b) The charge distribution of the  $C_2S_2$  at the  $\Gamma$  point for different energy levels. (c) The band alignment between the core and shell regions.

The band structure of a representative  $C_2S_2$  CSNW is shown in Figure 2a, which shows direct band gap at the  $\Gamma$  point. The energy levels near the band gap  $E_g$  are discrete, which suggests additional confinement in the core or shell region. The confinement effect can be confirmed by examining the charge distributions of these discrete states near the gap. Figure 2b shows the charge distributions of the conduction band minimum (CBM) and valence band maximum (VBM) states of  $C_2S_2$  CSNW at the  $\Gamma$  point. The charge of CBM state has mainly distributed in the shell while that of VBM state is in the core. Based on PDOS analysis, the VBM mainly originates from the  $4p$  states of the As atoms in the core region. But the CBM mainly consists of the  $4p$  states of the edge As and Ga atoms and  $4s$  states of other atoms in the shell region. The interactions between  $s$  and  $p$  states result in the dispersion of the CBM and VBM. Thus, free electrons are essentially confined in the GaAs-shell while free holes are kept in the InAs-core.

The operational band offset of the CSNWs is estimated by scanning the energy levels at the  $\Gamma$  point, following previous works [28]. The energy levels above the CBM are sequentially denoted as CBM+1, CBM+2, etc. A similar method is used to denote the energy levels below the VBM (VBM-1, VBM-2, etc). Moving up the energy levels from CBM to CBM+1 with a conduction band offset  $E_c$  leads to that the charge state is no more confined in the shell (Figure 2b). Similarly, Figure 2b shows the valence band offset between VBM-1 and VBM ( $E_v$ ). Since  $E_c$  and  $E_v$  are energy differences, the error due to the self-energy correction should be little although the error of DFT-calculated band gap is evident. In light of Figure 2b,  $E_c = 0.30$  eV and  $E_v = 0.19$  eV for  $C_2S_2$ . The corresponding band alignment of  $C_2S_2$  is plotted in Figure 2c, which shows a type-II band alignment.

The band gap of the  $C_2S_2$  nanowire is 0.79 eV based on the DFT calculations. It is well known that the DFT method always underestimates the band gap due to the self-energy correction. There are several accurate methods like GW to give a more realizable value, but it costs too much for our large system. To simplify, we adopt scissors operator [29] correction to overcome this problem. The DFT based band gaps of bulk InAs and GaAs are 0 and 0.52 eV, while the corresponding experimental band gaps are 0.54 and 1.51 eV. The energy differences between DFT calculated and experimental band gaps are 0.54 and 0.99 eV for bulk InAs and GaAs, respectively. Based on the Vegard's law [30-32], the value of scissors-corrected band gap for the CSNWs are determined by the following equation,

$$E'_g = E_g + 0.54 \times n_{\text{InAs}} + 0.99 n_{\text{GaAs}} \quad (1)$$

Where  $E'_g$  is the scissors-corrected band gap of the CSNWs,  $n_{\text{InAs}}$  and  $n_{\text{GaAs}}$  are the ratio of InAs and GaAs atomic pairs in CSNWs, respectively. The corrected band gaps for the core/shell nanowires are listed in Table 1. It is reported that the optimum band gap for a single-junction solar cell is close to 1.5 eV [33,34]. Therefore, the studied CSNWs are good candidates for the solar cell due to the suitable band gap and separated carriers.

Table 1. The axial lattice constant  $c$ , conduction band offset  $E_c$ , valence band offset  $E_v$ , and band gap  $E_g$  for the InAs/GaAs CSNWs with different radius based on the DFT calculations. The revised band gap  $E'_g$  and the value of scissors are also shown in the table.

	$c$ (Å)	$E_c$ (eV)	$E_v$ (eV)	$E_g$ (eV)	$E'_g$ (eV)	Scissors (eV)
C <sub>2</sub> S <sub>1</sub>	6.886	0.38	0.16	0.95	1.74	0.79
C <sub>2</sub> S <sub>2</sub>	6.779	0.30	0.19	0.79	1.67	0.88
C <sub>2</sub> S <sub>3</sub>	6.724	0.20	0.17	0.73	1.65	0.92
C <sub>3</sub> S <sub>2</sub>	6.850	0.31	0.16	0.54	1.37	0.83

To assess the impact of external axial strain on the band offset of the InAs/GaAs CSNWs, we have calculated the band structure and the edge state distributions of the C<sub>2</sub>S<sub>2</sub> under different strain levels. Based on the relaxed configuration of the C<sub>2</sub>S<sub>2</sub>, we apply axial tensile strain/compressive strain  $\epsilon$  by scaling its axial lattice constant. The applied strain varies from -3.5% to 4.5% and the variation of band offsets were plotted in Figure 3a. The prominent feature for the conduction band offset is that the compression decreases the  $E_c$  monotonically, in particularly, the  $E_c$  is even vanished for a compression larger than -2.6%; the tension firstly increases the  $E_c$  from 0.30 eV to 0.40 eV, then the  $E_c$  keeps almost constant. The above phenomenon suggests that the tension benefits the location of shell electrons while the compression is in contrast.

The valence band offset shown in Figure 3a also varies significantly with the applied axial strain: the tension decreases the  $E_v$  monotonically and the  $E_v$  is vanished for a tension larger than 3.9%; the compression firstly increases the  $E_v$  from 0.19 eV to 0.29 eV, then the  $E_v$  keeps almost constant. Thus the compression benefits the location of core holes while the tension is in contrast. Generally speaking, the charge carriers in C<sub>2</sub>S<sub>2</sub> nanowire can be separated when the applied strain is in the range of -2.6% to 3.9%, which is important for the application of solar cells. In addition, the strain-sensitive effect of band offsets in CSNWs suggests the possibility of strain sensors in nanosized devices because the corresponding electrical current crossing the radial heterojunction can be turned on or off by tailoring band offsets.

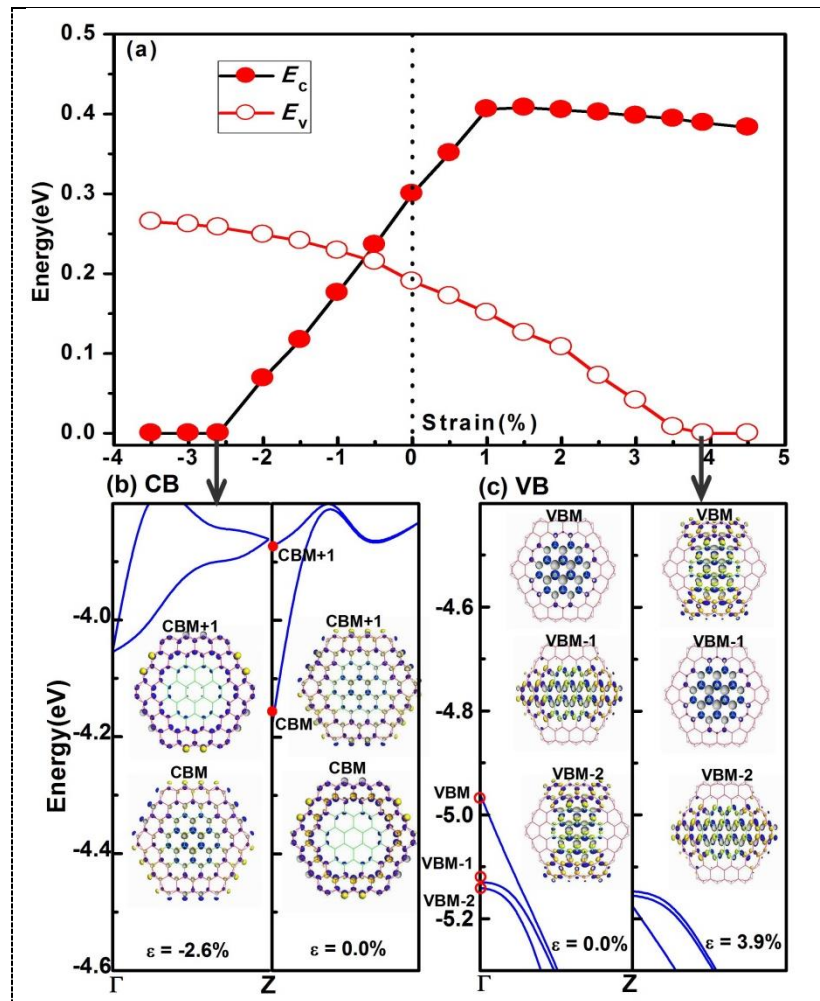


Figure 3. (a) Conduction band offset  $E_c$  and valence band offset  $E_v$  of  $C_2S_2$  CSNW as a function of the applied axial strain. (b) Conduction band structure of the  $C_2S_2$  CSNW under compressive strain and the corresponding charge distributions of the CBM and CBM+1 states. (c) Valence band structure of the  $C_2S_2$  CSNW under tensile strain and the corresponding charge distributions of the VBM, VBM-1 and VBM-2 states.

The mechanism contributing to the above changes in band offset of  $C_2S_2$  is the different response of energy levels at the  $\Gamma$ -point to the applied strain. We study the response of the CBM and CBM+1 levels to the tension. As shown in Figure 3b, the energy difference between CBM and CBM+1 decreases with the increasing compression. When the compression is larger than 2.6%, the CBM+1 surpasses the original CBM and becomes the lowest conduction state, making the conduction band offset zero accordingly. Moreover, this different response to the applied tension is also observed for the VBM, VBM-1 and VBM-2 states. As shown in Figure 3c, the energy difference between VBM and VBM-1 and that between VBM-1 and VBM-2 decrease with increasing tension. The VBM-2 surpasses the VBM-1 when the tension is larger than 2.5%, being the first nonconfined state. The energy difference between VBM and the new VBM-1 decreases with further increasing tension. The new VBM-1 surpasses the original VBM and becomes the highest valence state at tension larger than 3.9%, causing the zero valence band offset. The above different responses of energy levels near the gap to the applied strain explained the zero band offset discovered in Figure 3a.

The variation of the band gap  $E_g$  of  $C_2S_2$  CSNW under axial strain was plotted in Figure 4a. Interestingly,  $E_g$  keeps almost constant in the strain range of -2.6% to 3.9%, corresponding to the vanishing of  $E_c$  and  $E_v$  in Figure 3. However,  $E_g$  decreases significantly out of this range and it



decreases faster under compression. We plot the CBM and VBM to explain this variation, as shown in Figure 4b. In the range of -2.6% to 3.9%, the CBM and VBM decrease under tension (increase under compression) with the same amplitude, making  $E_g$  almost constant. When the tension is larger than 3.9%, the new VBM state shown in Figure 3c is insensitive to the strain while the CBM state still decreases with increasing tension, causing the decrease of  $E_g$ . When the compression is smaller than -2.6%, the VBM state still increases while the new CBM state (see Figure 3b) decreases with increasing compression, causing the faster decrease of  $E_g$  than that under tension.

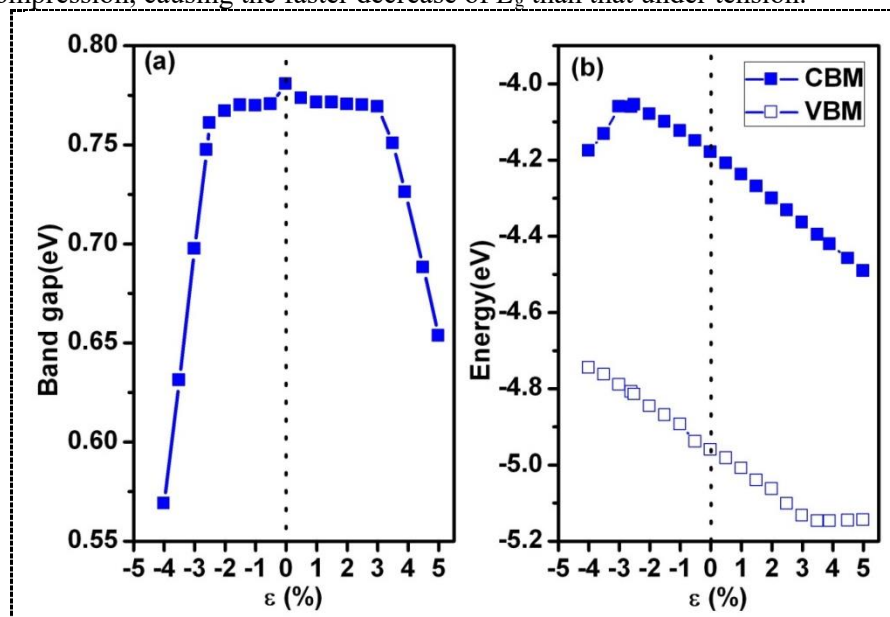


Figure 4. (a) Band gap  $E_g$  of  $C_2S_2$  CSNW as a function of the applied axial strain. (b) CBM and VBM of  $C_2S_2$  CSNW as a function of the applied axial strain.

#### 4. Conclusion

In summary, we have performed first principles calculations on InAs/GaAs CSNWs along the [0001] direction. Natural charge spatial separation was found due to the band offset. The band offsets were significantly modified by external axial strain.  $E_c$  increases under tensile strain while diminishes under compressive strain. In contrast,  $E_v$  diminishes under tensile strain while increases under compressive strain. The band gap  $E_g$  keeps almost constant in the strain range of -2.6% to 3.9% while it decreases significantly out of this range. Our results may be of practical interest for the nanodevices applications.

#### Acknowledgements

We acknowledge supports by the Fundamental Research Funds for National Natural Science Foundation of China (Grant No. 21703052), the Central Universities (Grant Nos. 2017B12914), China Postdoctoral Science Foundation (2015M571652). ZA acknowledges the financial supports from National Natural Science Foundation of China (Grant No. 21607029, 21777033), Science and Technology Program of Guangdong Province (2017B020216003), and Science and Technology Program of Guangzhou City (201707010359), “1000 Plan” for Young Professionals Program of China, “100 Talents” Program of Guangdong University of Technology.

#### Reference

- [1] Yao M Q, Huang N F, Cong S, Chi C Y, Ashkan Seyedi M, Lin Y T, Cao Y, Povinelli M L, Daniel Dapkus P and Zhou C W 2014 *Nano Lett.* **14** 3293
- [2] Yao M, Cong S, Arab S, Huang N, Povinelli M L, Cronin S B, Dapkus P D and Zhou C 2015 *Nano Lett.* **15** 7217
- [3] Wu D, Tang X H, Wang K and Li X Q 2017 *Sci. Rep.* **7** 46504

- [4] Zhang W, Zeng X L, Su X J, Zou X S, Mante P A, Borgström M T and Yartsev A 2017 *Nano Lett.* **7** 4248
- [5] Levinshtein M E and Rumyantsev S L 1996 *Handbook Series on Semiconductor Parameters* (U.K., London:World Scientific)
- [6] Paladugu M, Zou J, Guo Y N, Zhang X, Joyce H J, Gao Q, Tan H H, Jagadish C and Kim Y 2009 *Nanoscale Research Letters* **4** 846
- [7] Kavanagh K L, Salfi J, Savelyev I, Blumin M and Ruda H E 2011 *Appl. Phys. Lett.* **98** 152103
- [8] Biro R P, Kretinin A, Huth P V and Shtrikman H 2011 *J. Cryst. Growth* **11** 3858
- [9] Galicka M, Bukala M, Buczko R and Kacman P 2008 *J. Phys.:Condens. Matter* **20** 454226
- [10] Rosini M and Magri R 2010 *ACS Nano* **4** 6021
- [11] Shiri D, Kong Y, Buin A and Anantram M P 2008 *Appl. Phys. Lett.* **93** 073114
- [12] Zhang F, Crespi V H and Zhang P H 2009 *Phys. Rev. Lett.* **102** 156401
- [13] Li S, Jiang Q and Yang G W 2010 *Appl. Phys. Lett.* **96** 213101
- [14] Sadowski T and Ramprasad R 2010 *J. Phys. Chem. C* **114** 1773
- [15] Huang S T and Yang L 2011 *Appl. Phys. Lett.* **98** 093114
- [16] Hohenberg P and Kohn W 1964 *Phys. Rev.* **136** B864
- [17] Kohn W and Sham L J 1965 *Phys. Rev.* **140**, A1133
- [18] Delley B 1990 *J. Chem. Phys.* **92** 508
- [19] Delley B 2000 *J. Chem. Phys.* **113** 7756
- [20] Payne M C, Teter M P, Allan D C, Arias T A and Joannopoulos J D 1992 *Rev. Mod. Phys.* **64** 1045
- [21] Delley B 2002 *Phys. Rev. B* **66** 155125
- [22] Koelling D D and Hartreemon B N 1977 *J. Phys. C* **10** 3107
- [23] Perdew J P and Wang Y 1992 *Phys. Rev. B* **45** 13244
- [24] Galicka M, Bukala M, Buczko R and Kacman P 2008 *J. Phys.:Condens. Matter* **20** 454226
- [25] Shtrikman H, Popovitz-Biro R, Kretinin A, Houben L, Heiblum M, Bukala M, Galicka M, Buczko R and Kacman P 2009 *Nano Lett.* **9** 1506
- [26] Joyce H J, Wong-Leung J, Gao Q, Tan H H and Jagadish C 2010 *Nano Lett.* **10** 908
- [27] Martelli F, Rubini S, Piccin M, Bais G, Jabeen F, De Franceschi S, Grillo V, Carlino E, D'Acapito F, Boscherini F, Cabrini S, Lazzarino M, Businaro L, Romanato F and Franciosi A 2006 *Nano Lett.* **6** 2130
- [28] Jiang Q G, Wen Z and Q. Jiang 2012 *Solid State Commun.* **152** 2120
- [29] Levine Z H and Allan D C 1991 *Phys. Rev. B* **43** 4187
- [30] Said A, Debbichi M and Said M 2016 *Optik* **127** 9212
- [31] Gorczyca I, Lepkowski S P, Suski T, Christensen N E and Svane A 2009 *Phys. Rev. B* **80** 075202
- [32] Zhang M and Li X 2017 *Phys. Status Solidi B* **254** 1600749
- [33] Blom P W M, Mihailetchi V D, Koster L J and Markov D E 2007 *Adv. Mater.* **19** 1551
- [34] He Z C, Xiao B, Liu F, Wu H B, Yang Y L, Xiao S, Wang C, Russell T P and Cao Y 2015 *Nature Photonics* **9** 174